Comparative Study of Strain-Gauge Balance Calibration Procedures Using the Balance Calibration Machine

I. Philipsen[1]
German-Dutch Wind Tunnels (DNW), 8300 AD Emmeloord, The Netherlands

and

J. Zhai[2]
German-Dutch Wind Tunnels (DNW), 51147Köln, Germany

A new balance calibration load table was designed and validated using the Balance Calibration Machine (BCM). Three load tables were used to calibrate the same new balance, a more traditional "One Factor At a Time" (OFAT) load table, an Modern Design Of Experiments (MDOE) structured load table and an MDOE randomized load table. The MDOE design is compared to other designs to analyze the properties of this load table design. The calibration results of all three load tables are tested against an independent set of check load points. It is demonstrated that the MDOE load table produces nearly identical results as the OFAT load table, but has a significant time gain and demands little of the capacity of the BCM.

Nomenclature

a_i	=	Accuracy coefficient of balance load component 'i' [-]
A_i	=	Offset coefficients [N, Nm]
A_{ij}	=	Linear coefficients [N/(mV/V), Nm/(mV/V)]
A_{ijk}	=	Quadratic coefficients [N/(mV/V)^2, Nm/(mV/V)^2]
b_i	=	Accuracy limit coefficient of balance load component 'i' [-]
F_i	=	Maximum load of a specific balance load component 'i'[N, Nm]
F_n	=	Actual load acting on balance load component 'n' [N, Nm]
$F_{n,\,max}$	=	Maximum load of balance load component 'n' [N, Nm]
F_1, F_x	=	Axial force [N]
F_2, F_y	=	Side force [N]
F_3, F_z	=	Normal force [N]
F_4, M_x	=	Rolling moment [Nm]
F_5, M_y	=	Pitching moment [Nm]
F_6, M_z	=	Yawing moment [Nm]
i	=	Index
R_i	=	Output reading of the balance (i=1,…,6) [mV/V]
V	=	Variance
x_0	=	A certain load condition of the balance (vector)
$\hat{y}$	=	Estimated response of the balance (vector)
X	=	Matrix of levels of independent variables
δ_i	=	Maximum error of balance load component 'i' [N, Nm]
σ	=	Standard deviation (in this case of the BCM)
σ_0	=	Standard deviation for a balance load component at a certain balance load condition x_0.

[1] Department Head, Instrumentation and Controls (INC), P.O. Box 175, AIAA Member
[2] Scientist, KKK, Linder Höhe.

I. Introduction

THE response signals of an internal strain gauge balance with an air-line bridge system, mounted to it, are not only dependent on the loads (forces and moments) applied to the balance, they are also affected by parasitic effects caused by the air-line bridge system. This implies that the calibration of the balance without the air-line bridge system is no longer valid and has to be corrected. For instance, an air-line bridge system will introduce additional stiffness to the balance or pressure in the air-line bridge system may lead to an offset of the response signals. All the parasitic effects have to be calibrated, leading to an elaborate and time consuming process to achieve accurate balance results[2]. Calibration of these effects in an automatic BCM may shorten the time needed to obtain the required corrections, but would require a considerable amount of load points, since apart from the load an additional parameter, like e.g. the pressure in the air-line bridge system, has to be varied. Thus, this will have financial consequences. In an effort to reduce the number of load points, required for a calibration, this study was initiated. Another consideration for this study is that when we can obtain a balance calibration with considerably less load points, the labor-intensity of a manual balance calibration will be reduced and it will become more feasible again to do such a manual balance calibration.

The study is split in two phases. The aim in the first phase is, to design a load table with considerably less load points without decreasing the quality of the calibration results at the same time. Thus opening up the possibility to save time on a calibration, or have the opportunity to vary an additional parameter (e.g. the pressure in an air-line bridge system), or make the calibration work less labor-intensive. In a second phase, this type of load table design could then be used to design a load table for an actual calibration of e.g. a balance with an air-line bridge system. The first phase of this study is now concluded and the results are presented in this paper.

II. Approach

Based on the reported success with the single vector system[3], an MDOE-like approach was adopted to design two alternative load tables for a balance calibration. As starting point in this study, the math model used to describe the behavior of the internal strain gauge balance, is assumed to be valid. The math model used at DNW is described by the following equation:

$$F_i = A_i + \sum_{j=1}^{6} A_{ij} R_j + \sum_{j=1}^{6} \sum_{k=j}^{6} A_{ijk} R_j R_k \tag{1}$$

In general, the calibration is determined knowing the natural zeros of the balance and all loads (including the ones caused by e.g. the mass of calibration bodies) acting on the balance. Therefore, the term A_i is often not fitted and is set to zero for most calibrations.

Given this math model three calibration load tables are designed. The first one can best be described as a OFAT design load table. The second and third are designated MDOE structured and MDOE randomized, respectively. These load tables both have considerably less load points than the OFAT load table. The MDOE load tables consist of all maximum load points out of the OFAT load table with additional zero load points. The MDOE randomized is an MDOE structured load table, randomized in sequence. This load table is used to investigate the effect of randomization on the calibration results. All three load tables are used to calibrate a new balance in the QinetiQ BCM. In addition to the calibration load tables, a set of independent load check points is measured to validate the calibration results. All load points are measured within a period of three days form the 3rd to the 5th of May 2006.

The validity of the calibration is checked by analysis of the residuals. The residuals are analyzed for each calibration load table individually, as well as for the check load points. All residuals should be within the set accuracy limits of the calibrated balance. The accuracy for DNW-LLF (German-Dutch Wind Tunnels – Large Low-Speed Facility) balances is defined according to the following equation:

$$\delta_i \le \frac{1}{1000} \cdot |F_i| \cdot \left[a_i + \sum_{\substack{n=1 \\ n \neq i}}^{6} \left| \frac{F_n}{F_{n,max}} \right| \right] \le \frac{1}{1000} \cdot b_i \tag{2}$$

This equation describes the maximum error for each load component of the balance as function of a set of coefficients and the actual load acting on the balance. This formulation accounts for the fact that the balance

accuracy is affected by the number of loads acting on the balance as well as by the load level of these loads. For the new balance the target accuracy coefficient (a_i) for all individual load components is 1. This corresponds to an accuracy of 0.1% full scale. Also the target accuracy limit coefficient (b_i) is 1. The accuracy coefficients are listed in Table 2 for a number of LLF balances.

Furthermore, the frequently measured zero load points are used to verify the repeatability of the balance. This should be about 1/3 of its accuracy limit. Finally, the matrix coefficients themselves are evaluated. Depending on the time between the calibrations the main coefficients, should not change more then 0.3% at the maximum when the balance has not been calibrated for a long time.

III. Calibration

A. Background

When considering internal stain gauge balances in use at a large low-speed wind tunnel, it is imminent that we are dealing with what can best be described as big balances[1]. These internal strain gauge balances are of considerable size (e.g. balance W608 has a length of 1000 mm and a diameter of 224 mm) and load range. The load range of internal balance W608 is presented in Table 1. Note that the large model weight leads to the requirement of a relatively large axial load range. Calibration of big internal balances is traditionally a time-consuming elaborate job, due to the large amount of dead weights that need to be handled. Therefore, big balances are calibrated less regularly than smaller sized/ranged balances. In an effort to calibrate big balances more regularly, DNW utilizes the QinetiQ BCM. This BCM is unique by the fact that it is large enough in size and load range to handle a big balance.

Overtime the load table design for the BCM evolved. The first load table, in 1998, is set-up to simulate a dead weight calibration (SDW) with additional points for some load combinations that are too difficult for a manual calibration (e.g. it is very hard to apply a combination of two pure moments in a dead weight calibration). In 2001 the load table is a “One Factor At a Time” design with additional independent load check points. This latter load table design is the baseline load table design in this study and is described in more detail in section III C. The SDW calibration load table has about 1200 load points and is represented graphically in Fig. 4; the OFAT load table has 734 load points and is represented graphically in Fig. 5. Also the progress in computer performance made it possible to advance in the method used to determine the actual calibration coefficients. This changed from an iterative matrix inversion process to a direct fit using the global regression method.

B. Balance B667

The balance used for this study is a new internal strain gauge balance that is especially suited for propulsion simulation testing with LLF-size wind tunnel models at Mach numbers up to about 0.4. This six-component internal strain gauge balance, designated B667, is a moment type of balance, designed and manufactured by the NLR, see Fig. 1. The balance has a diameter of 135 mm, inclusive the heat shield and has a length of 520 mm. The balance center is defined at 260 mm downstream of the metric flange. The moment sections are 160 mm up- and downstream of the balance center. The load range of this balance is given in Table 1. For all components the maximum single load is equal to the maximum loads as listed in Table 1. At 90% of the maximum load range all loads may occur simultaneously. The loads are defined according to the DNW sign convention for balance loads as shown in Fig. 1. It should be noted that this is a moment type of balance and not a direct read balance and should therefore not be treated as one.

C. Balance Calibration Machine

The BCM was mainly designed for the calibration of the large internal sting-mounted balances used at the 5 m tunnel (QinetiQ, Farnborough). It was developed from an earlier smaller machine, and has been used successfully for 30 years with both sting balances and under-floor balances; see Fig. 2 and Fig. 3. A feature of the BCM is that the correct geometry of the calibration load system relative to the balance is maintained throughout the calibration, by automatic repositioning of the load system to follow balance deflection under load.

The calibration loads (forces and moments) are produced by the controlled action of six special bi-directional pneumatic piston/cylinder assemblies, called force generators (FGs), driven by Ruska pressure controllers. The weight of the loading tree is compensated by an adjustable counterbalance lever and weight system; nevertheless, when the balance deflects, tare forces of the system are affecting the balance. The nominal maximum capacity of the BCM is presented in Table 3. To allow for good results over various calibration ranges, FGs are available in four sizes, nominally 10, 20, 50 and 100 kN full scale. This also helps to prevent overloading. The BCM load range used for this calibration is also presented in Table 3.

The mechanical behavior of the FGs is standardized for both, their use and their calibration; thus inaccuracies due to e.g. seal effects are largely eliminated. Calibrations of the FGs show that they are accurate in converting applied pressures into values of calibration force, typically within 0.003% of full scale.

In using the BCM to generate a typical calibration load, these small inaccuracies in the FGs will combine with small inaccuracies in the Ruska pressure controllers, in the BCM geometry and in the weight counterbalance. Calibration loads seem typically to be accurate to 0.01% of BCM full scale. As many of the inaccuracies are load-dependent, the absolute inaccuracy will reduce with smaller loads. Therefore, when calibrating a balance of load range of B667, we believe the typical error in calibration load is less than about 0.03% of the balance's full scale.

To establish confidence in the performance of the BCM, two calibrations are compared to an initial dead weight calibration. The difference in the main matrix coefficients is shown in Fig. 6 for two calibrations of balance W608. The minimum time between two of these calibrations is five years, so we may expect differences between the coefficients up to the set limit of 0.3%. The differences are limited to 0.3%, so both BCM calibrations compare well with the initial dead weight calibration.

D. Load Table Design

This section describes how the three load tables used for this calibration OFAT, MDOE structured and MDOE randomized are designed. These load tables are graphically represented in Fig. 5.

The OFAT load table starts off with a first order calibration of pure loads for forces as well as for moments. For each positive load component individually, loads are applied from 0% in steps of 10% to 100% full scale and on the way back form 95% in steps of -10% through to 5% full scale. An identical procedure is followed for each negative load component. For the second order calibration, the following calibration procedure is adopted. For all fifteen combinations of two loads, combined loads are applied. First, one load component is held constant at +75% of its load range and the other load component is varied from 0 to +75% and from 0 to -75% of its load range. Then the one load component is held constant at -75% of its load range and the other load component is varied from 0 to +75% and from 0 to -75% of its load range. After this the second load component is held constant at +75% and -75% of its load range and the first load component is varied from 0 to +75% and from 0 to -75% of its load range. The number of load points are chose in such away that the first order calibration takes about 1/3 of the total number of load points and the second order calibration thus 2/3 of the total number of load points. Overall, the first order calibration consists of 253 load points and the second order calibration consists of 481 load points. In total 734 load points are used for the OFAT load table.

The MDOE load tables consist of 101 to 103 load points. These load tables were devised out of convenience and are not optimized in any way. Only after the calibration a more detailed and thorough analysis of these MDOE load tables was performed according to the theory presented in Ref. 4. In the math model used to describe the behavior of the balance (Eq.1), the offset term is not fitted in general. In order to fit this term, the natural zeros or the mass of the balance's weighted part has to be known. If we want to fit this math model using a pure force or moment calibration, we need at least three points. These are chosen in such away that the influence of load errors on the slope fit should be minimal. Chosen are the points -100%, 0 and 100% of the full scale load. To fit the combination terms we only need one combined load point for each load combination. However, from experience we now that the behavior of a moment type of balance is not always consistent in magnitude in all four quadrants. Therefore we take a combined load point in each quadrant to fit only the consistent part of the behavior and make the fit more robust. The combined 100% full scale load points are not always possible for each combination due to the maximum load limit of the balance. Preferably, we would therefore have used a constant load vector. So, the combination load point would have been at $\frac{1}{2}\sqrt{2}$ of the single component maximum load. Using load points that are part of the OFAT load table makes it more transparent to compare results, therefore we chose 75% full scale load on each component. Finally, extra zeros were added to gain insight in the hysteresis and repeatability of the balance and BCM.

Further analysis of the MDOE load table design shows that the design we use is a modified face-centered central composite design (CCD). It contains all the factorial designs from the combination of every two variables, augmented with a group of star points. To have a better understanding of the properties of the MDOE load table design, we compared this design with our original OFAT design, the standard CCD design and a D-optimized design (D-Opt). We calculated the standard deviation of the predictions with the following equation[4]:

$$\sigma_0 = \sqrt{V[\hat{y}(x_0)]} = \sigma\sqrt{x_0'(X'X)^{-1}x_0} \tag{3}$$

This equation describes the standard deviation at a given load condition of the balances (σ_0) as function of the standard deviation of the calibration system (σ), the load condition on the balance (x_0) and the load table design (X).

In our case σ is the standard deviation of the BCM. To simplify the comparison, its value is assumed to be 1. For the results presented here the math model included the offset term A_i.

Fig. 7 shows the standard deviation of the prediction when F_1 is varied and $F_2 = F_3 = F_4 = F_5 = F6 = 0$ ($x_0 = [F_1, 0, 0, 0, 0, 0]$). It is evident that for a single component calibration the MDOE load table performs comparably to the CCD design. The standard deviations of the prediction when F_1 and F_2 are varied and $F_3 = F_4 = F_5 = F6 = 0$ is presented for the different load table designs in Fig. 8 to Fig. 15 ($x_0 = [F_1, F_2, 0, 0, 0, 0]$). It is clear that the standard deviation of the calculated components is very small in the range $|F_i| \leq 50\%$. It is about 0.2 σ. Furthermore, we see that the MDOE design is not exactly rotational, but the change of the prediction variance with direction is very small. This means that we have almost a unique standard deviation for all six components. Further analysis shows that the standard deviation of the perditions for the MDOE load table design is in general two times larger than the one for the OFAT load table. This is independent of the load level of the other components and the omission of the A_i term in the math model.

The advantage of the MDOE load table design is that the demand on the capacity of a calibration machine is small. Only the single component is loaded with the full scale loads and just a combination of two load components is needed in addition. The load for the combination cases is 75% of the full scale load. It has also become evident that for future calibrations we can adapt the load table design to our special needs. For example, if we need a unique accuracy over the whole load range, we can use the D-optimized design. This design has the property that the standard deviation is all most constant over the complete load range, it only varies between 0.7 and 0.8. If we want to reduce the number of calibration points, we can use the standard CCD or Box-Behnken design. The disadvantage of all these designs is that all six components must be loaded at the same time with full scale load. This may be a problem for some calibration machines and for some balances.

The MDOE randomized load table is essentially the same as the MDOE structured load table, apart from the fact that it is randomized. Unfortunately, during the randomization process a number of load points were omitted and replaced with a zero load point. The -100% load points of the single components were replaced by a zero load point for all but the Fz component. Nevertheless, the load table proved to be very useful since the given math model could still be fitted.

To validate the obtained matrix coefficients, an independent set of load points is taken, consisting of load points that were not part of any of the load tables. Since the BCM allows simultaneous application of six load components, it was used to simulate a wind tunnel measurement of a typical LLF model scaled to the range of this balance[2]. The simulated conditions represented a weight polar, a pitch polar, a yaw polar, the maximum load condition and a repetition of the yaw polar. The load table was finally ended with a repetition of the single component first order calibration of the axial component. The maximum load point is the maximum simultaneous load condition, 90% of the FS load range on all six components.

E. Data Reduction

The recorded balance signals and loads are pre-processed before the balance calibration matrix is determined. During this pre-processing several corrections are applied.

The loads applied to the balance are corrected for tare-forces due to the weight of the loading tree. On the metric end of the loading tree two inclinometers are installed. These inclinometers measure the roll and pitch angles of the metric side of the balance. The weight tares are rotated over roll and then pitch to the metric axis system.

The zero signals of the balance are recorded before the balance is mounted to the BCM. This zero represents a situation, where the balance is mounted to a sting and no loads are applied to the balance (only the weighted part of the balance, the adapters, the BCM mounting block and the electronic offset are measured by the gauges).

When the balance is mounted in the BCM, the loading tree is positioned in such away that the signals of the balance correspond to the previously recorded zero. The then recorded zero is subtracted from all further recorded signals. Further, the supply voltage is measured for each data point. The balance output signals are corrected for deviations to the nominal supply voltage of 10V. This is done for each output signal individually. Finally, the output signals are made ‘non-dimensional’ with the nominal supply voltage of 10V.

The matrix coefficients in Equation 1 are determined using global regression.

IV. Results

The difference in the main linear matrix coefficients, with respect to the OFAT matrix, is presented in Fig. 16 for both MDOE matrices. We see that the difference for the main matrix terms is very small. The differences with respect to the matrix out of the OFAT load table are on average below 0.05%. Two terms clearly have a larger deviation, term A_{11} corresponding to the axial load and A_{56} contributing to the pitching moment. If we disregard

these two terms, the differences with respect to the matrix out of the OFAT load table are on average below 0.02%. Since these calibrations are direct-repeat calibrations it is fair to presume that the change in the coefficients should be better than the repeatability of the balance. The target accuracy for this balance is 0.1%, thus the target repeatability is 0.033%. So, the matrices compare very well apart for the terms A_{11} and A_{56}. The reason for this is the larger hysteresis in the balance for the two load components associated with these terms. Especially the axial component has a somewhat larger than normal hysteresis. The math model does not describe this hysteresis behavior of a balance. In the analysis of the results, the results for the axial component should therefore be treated with some reservation.

The standard deviation of the residuals is calculated twice for each of the three matrices. Once it is calculated for the corresponding load table and once for the check load points. The results are listed in Table 4 and presented in Fig. 17 and Fig 18. The overall standard deviation for the corresponding load tables is lower than the one for the check load points, as is to be expected since the matrices are a product of a data fit of the calibration load tables. The difference in standard deviation for the different load tables mainly originates from the axial component contribution. Excluding Fx from the overall standard deviation leads to comparable results for all three load tables. We can also conclude that the MDOE randomized load table generally leads to somewhat better results than the MDOE structured load table. Considering the facts, that the estimated standard deviation for the MDOE load table design is twice that of the OFAT load table design and the fact that the overall standard deviation is comparable for all three load tables, we can state that the MODE design has reached nearly the same accuracy as the OFAT design.

Comparing the maximum residuals for each component, see Table 5, Fig. 19 and Fig. 20, we see that the OFAT matrix has the largest errors within its corresponding load table and the smallest errors for the check points. Again the axial components behavior deviates from the other components in that it has larger errors. The Fx residuals are presented in Fig. 23 for the check load points. For clarity the balance loads of the check load points are presented in Fig. 22. It is clearly visible that the repeated pure load calibration of Fx at the end of the check points load table shows the signs of a relatively large hysteresis loop. This is further illustrated by the mean of the residuals over the check load points; see Table 6 and Fig. 21. It is negligibly small for all components apart from Fx. Furthermore, note that the maximum load point, number 53, clearly sticks out. Looking at the errors of Fz and Mz, Fig. 24 and Fig. 25, we see that other components perform better than the axial component. The maximum residual for Fz only occurs at the maximum combined load point.

For this new balance the accuracy coefficients have been determined using the OFAT matrix and all available load points. The coefficients are listed in Table 2. The balance meets the set target accuracy for all components excluding Fx. The performance of the Fx component is nevertheless good, the accuracy coefficient has a value of 1.2 which is still close to the target value of 1. Comparing the accuracy coefficients with the ones of other LLF balances it is clear that this balance has a state of the art performance.

Finally, it is interesting to note that the reduction in the number of load points is about 85%. This reduction in load table points cannot be fully converted to a time reduction since the BCM has to travel from one maximum load point to the next. Nevertheless, the reduction in time for the MDOE load tables is at least 75%.

V. Conclusion

This comparative study of calibration procedures has shown that it is possible to considerably reduce the number of load points required to obtain a valid calibration matrix. The new MDOE load table is designed with the assumption that the math model describing the balance behavior is valid. Verification of the validity of the matrices by using an independent data-set of check load points proves that despite the fact that the designed MDOE load table is not an optimized one, it produces nearly as accurate results as the larger OFAT load table. The time gain for the actual calibration is significant and can be up to 75%. The new MDOE load table has furthermore the advantage that the demand on the capacity of a calibration machine is low and the combined load cases are within the load rhombi of the balance.

Acknowledgments

The authors would like to thank Kees Bogers and Hanne ten Wolde for their efforts and contributions in the design, manufacturing and calibration of internal strain gauge balance B667.

References

[1]Graewe, E., Ewald, B. Eckert, D. “Design and Construction of Internal Balances for the German/Netherlands Wind Tunnel (DNW)”, 1st International Symposium on Strain Gauge Balance, 14 August 1997

[2]Philipsen, I., Hoeijmakers, H., Alons, H.J., "A New Balance And Air-Return Line Bridges For DNW-LLF Models (B664 / RALD 2001)", 4th International Symposium on Strain-Gauge Balances, San Diego, USA, 10–13 May 2004
[3]Parker, P.A., Morton, M., Draper, N., Line, W., "A Single-Vector Force Calibration Method Featuring the Modern Design of Experiments", 39th AIAA Arospce Science Meeting & Exhibit, Reno, Nevada, USA, 8–11 January 2001
[4]Montgomery, D.C., "Design and Analysis of Experiments", 5th edition. John Wiley & Sons, 2001

Table 1. Load range of balances.

Load	W608/B664	B667
F_x	20 [kN]	8 [kN]
F_y	12.5 [kN]	8 [kN]
F_z	50 [kN]	21 [kN]
M_x	9 [kNm]	5 [kNm]
M_y	16 [kNm]	6 [kNm]
M_z	9 [kNm]	4 [kNm]

Table 2. Accuracy coefficients (Equation 1). Based on OFAT matrix

Accuracy coefficients	Balance W608	Balance B664	Balance B667
a_{Fx}	1.5	0.6	1.2
a_{Fy}	1.7	1.0	1.0
a_{Fz}	1.3	0.5	0.8
a_{Mx}	1.5	1.0	0.6
a_{My}	1.0	0.6	0.7
a_{Mz}	1.0	0.5	0.7
b_{Fx}		2.0	2.1
b_{Fy}		2.0	1.2
b_{Fz}		2.0	0.8
b_{Mx}		2.0	0.7
b_{My}		2.0	1.0
b_{Mz}		2.0	1.0

Table 3. Load range BCM

Load	Maximum Range	Used Range
Fx	22 [kN]	20 [kN]
Fy	127 [kN]	20 [kN]
Fz	90 [kN]	90 [kN]
Mx	140 [kNm]	12.3[kNm]
My	15 [kNm]	15.0[kNm]
Mz	40 [kNm]	12.3[kNm]

Table 4. Standard deviation of the residuals

Load Points	Overall [%FS]	Excluding Fx [%FS]	Load table design	Fx [%FS]	Fy [%FS]	Fz [%FS]	Mx [%FS]	My [%FS]	Mz [%FS]
Calibration Points	0.026	0.019	OFAT	0.042	0.027	0.019	0.016	0.016	0.024
	0.026	0.021	MDOE Structured	0.038	0.035	0.020	0.015	0.018	0.023
	0.021	0.018	MDOE Randomized	0.027	0.029	0.018	0.013	0.017	0.020
Check points	0.031	0.022	OFAT	0.052	0.023	0.022	0.015	0.034	0.025
	0.040	0.024	MDOE Structured	0.079	0.028	0.030	0.016	0.032	0.025
	0.037	0.022	MDOE Randomized	0.074	0.022	0.029	0.015	0.030	0.021

Table 5. Maximum error in the residuals

Load Points	Load table design	Fx [%FS]	Fy [%FS]	Fz [%FS]	Mx [%FS]	My [%FS]	Mz [%FS]
Calibration Points	OFAT	0.160	0.118	0.076	0.066	0.088	0.075
	MDOE Structured	0.132	0.099	0.070	0.047	0.063	0.071
	MDOE Randomized	0.123	0.077	0.060	0.035	0.057	0.049
Check points	OFAT	0.185	0.066	0.062	0.044	0.100	0.060
	MDOE Structured	0.295	0.119	0.203	0.058	0.094	0.113
	MDOE Randomized	0.258	0.065	0.175	0.044	0.083	0.077

Table 6. Mean error in the residuals

Load Points	Load table design	Fx [%FS]	Fy [%FS]	Fz [%FS]	Mx [%FS]	My [%FS]	Mz [%FS]
Check points	OFAT	-0.060	-0.001	0.002	0.002	0.000	0.005
	MDOE Structured	-0.084	-0.008	0.009	0.000	-0.006	-0.005
	MDOE Randomized	-0.065	-0.002	0.009	0.001	-0.010	0.006

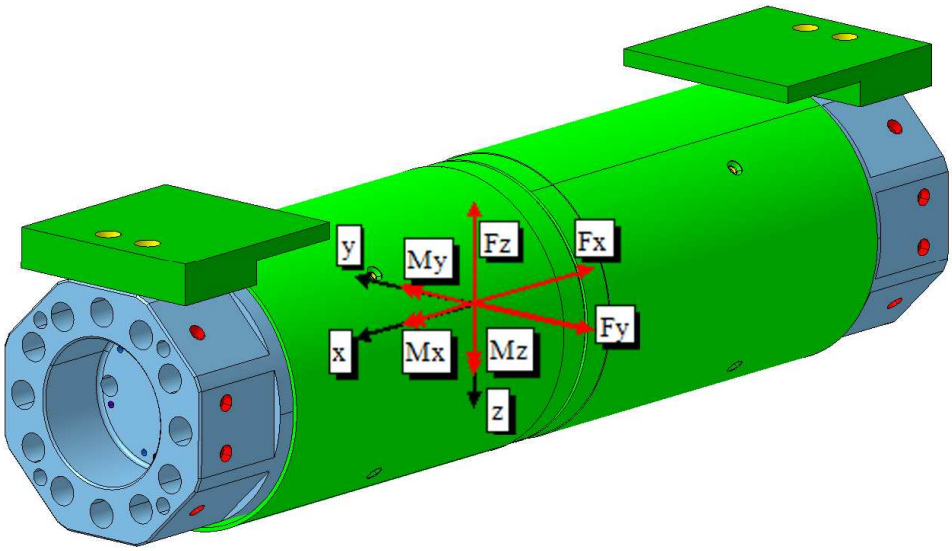

Figure 1. Balance B667, DNW sign convention

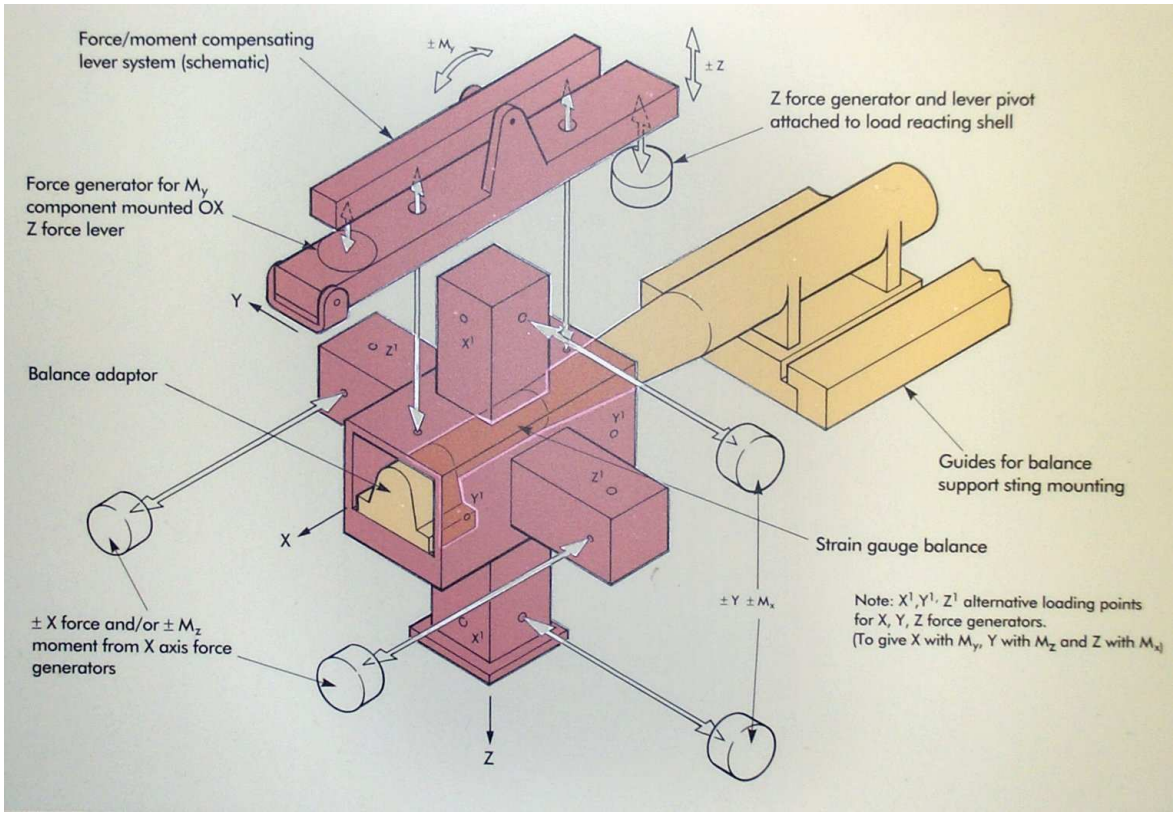

Figure 2. Schematic layout of the QinetiQ BCM. Note that the forces in the QinetiQ sign convention are opposite to the forces according to the DNW sign convention.

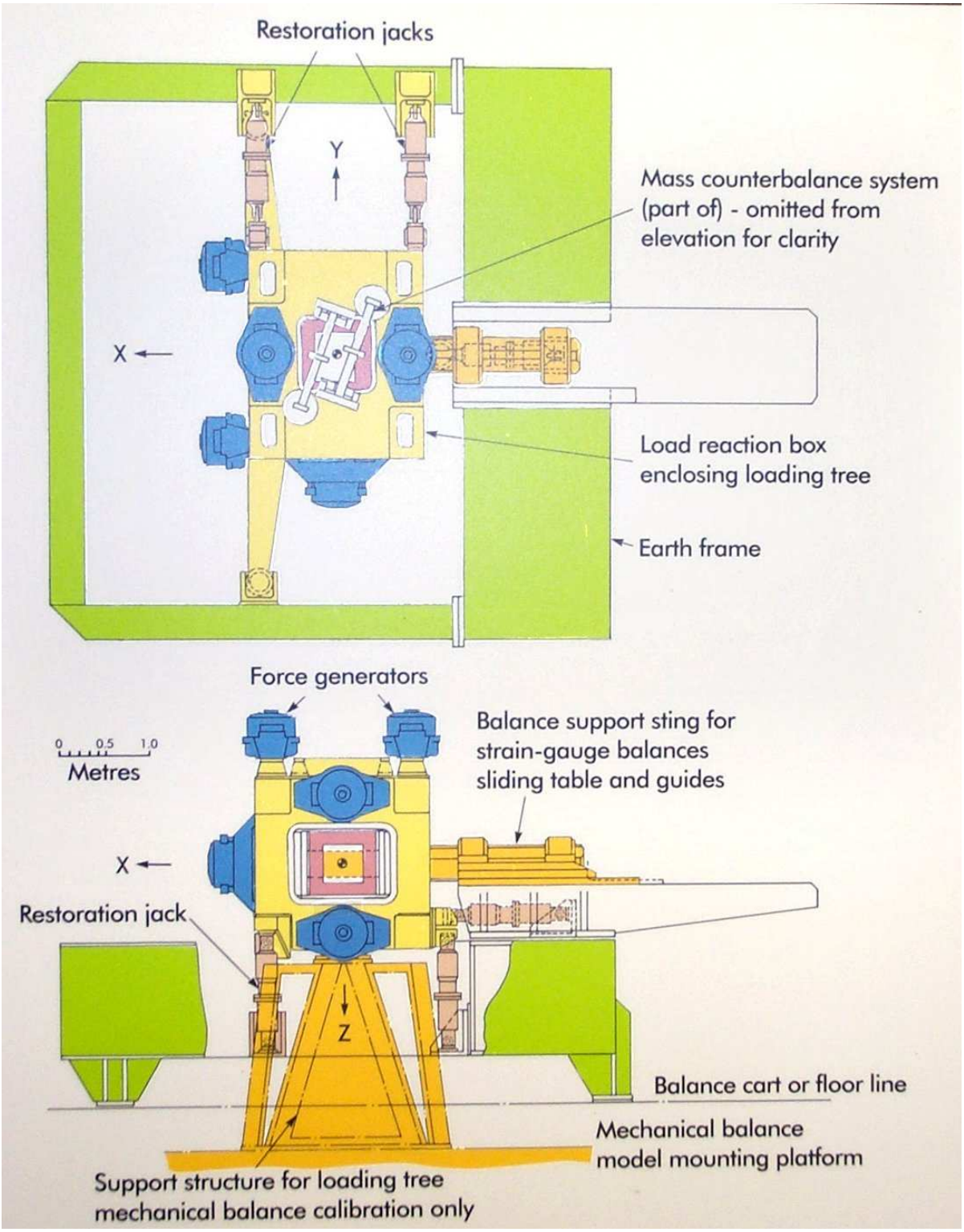

Figure 3. Sketch of the QinetiQ BCM

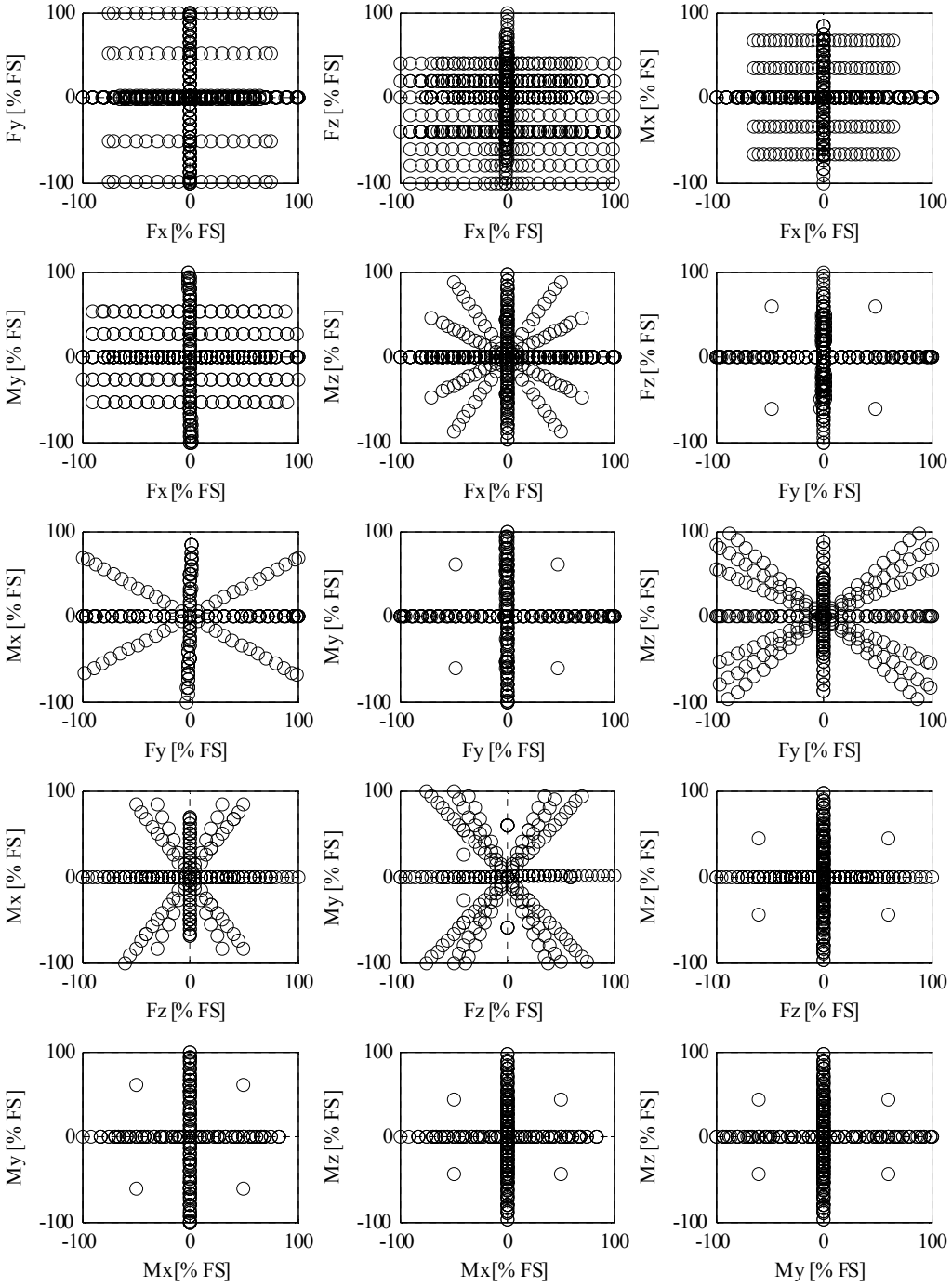

Figure 4. Simulated dead weight calibration load table.

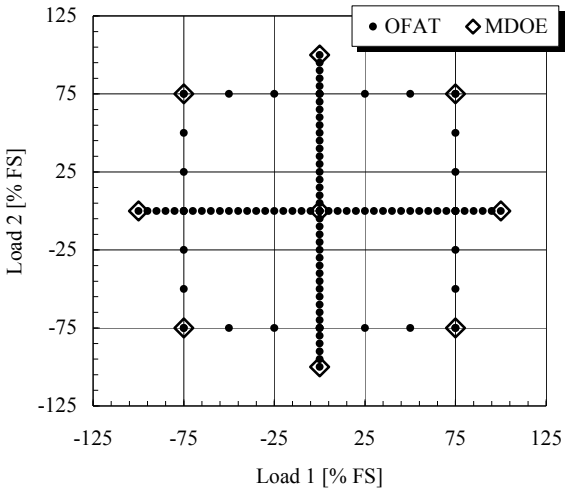

Figure 5. Load tables designs

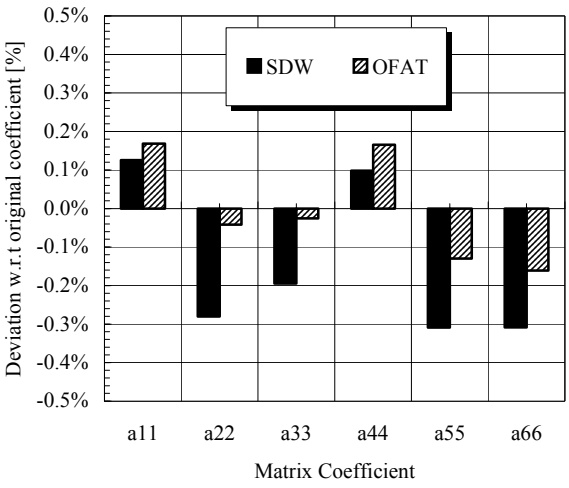

Figure 6. Change in matrix coefficients for two calibrations of balance W608

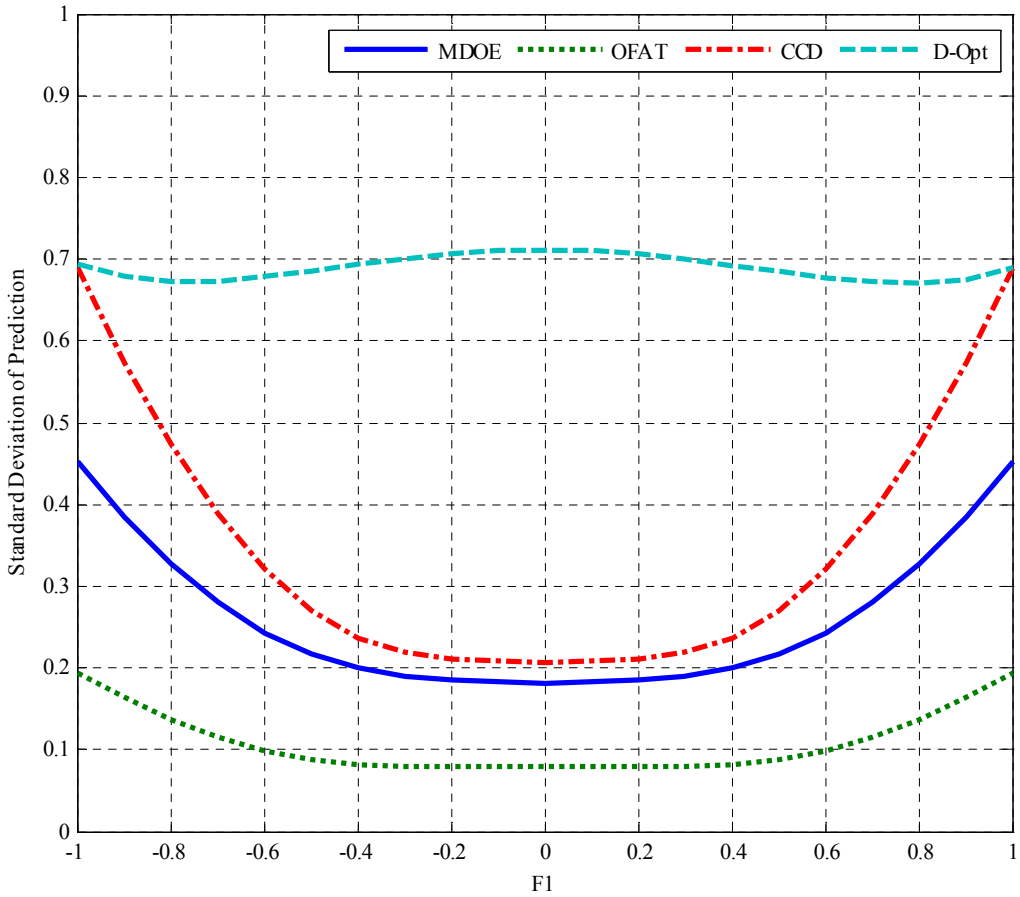

Figure 7. σ_0 curves for x_0 = (F1, 0, 0, 0, 0, 0)

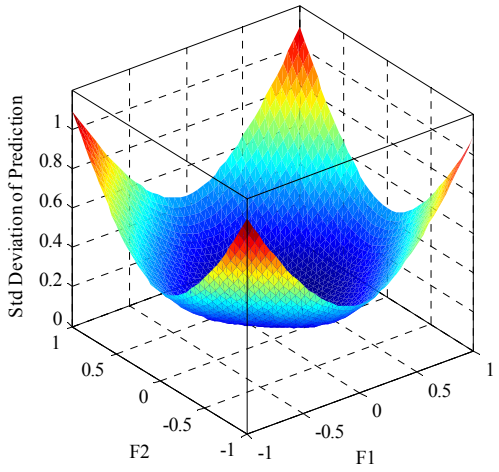

Figure 8. σ_0-surface for the MDOE load table

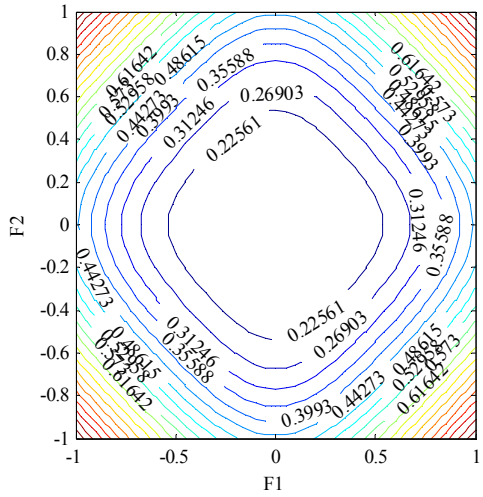

Figure 9. σ_0-contours for the MDOE load table

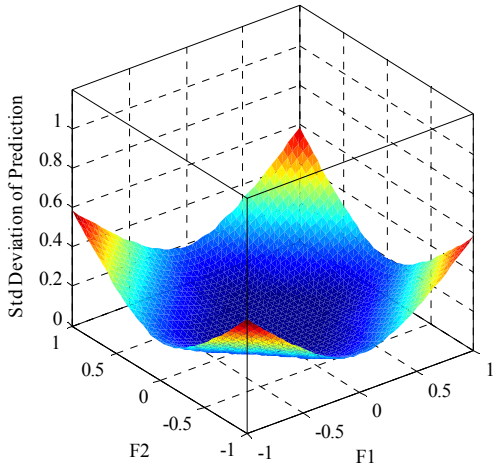

Figure 10. σ_0-surface for the OFAT load table

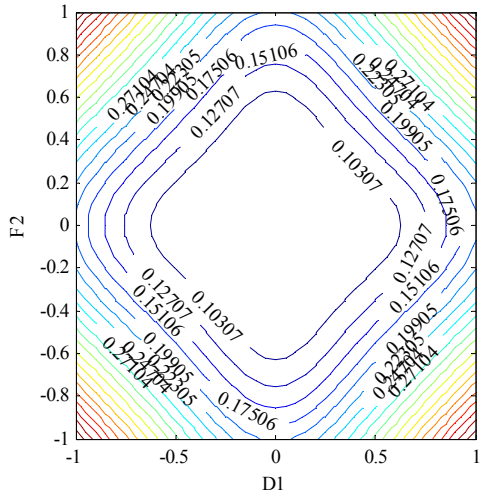

Figure 11. σ_0-contours for the OFAT load table

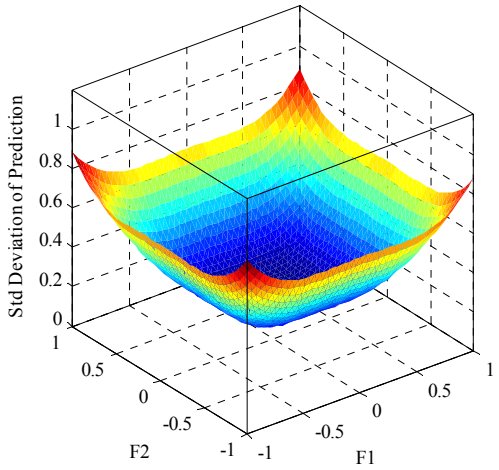

Figure 12. σ_0-surface for the CCD load table

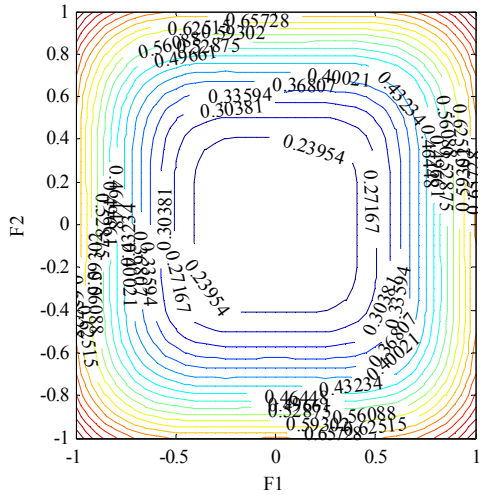

Figure 13. σ_0-contours for the CCD load table

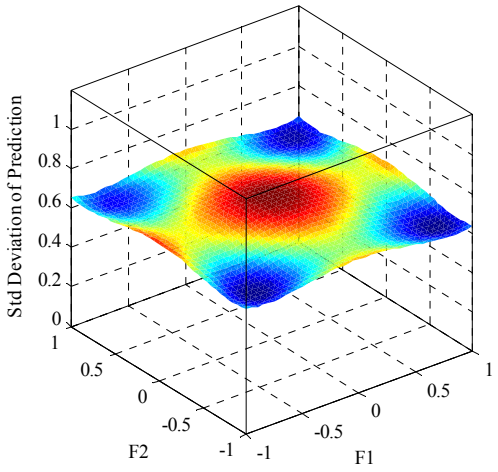

Figure 14. σ_0-Surface for the D-Opt load table

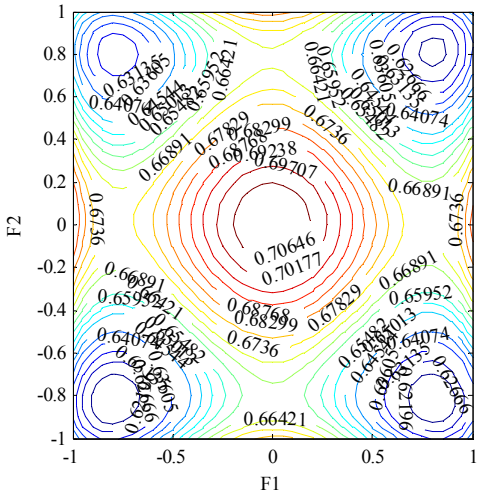

Figure 15. σ_0-contours for the D-Opt load table

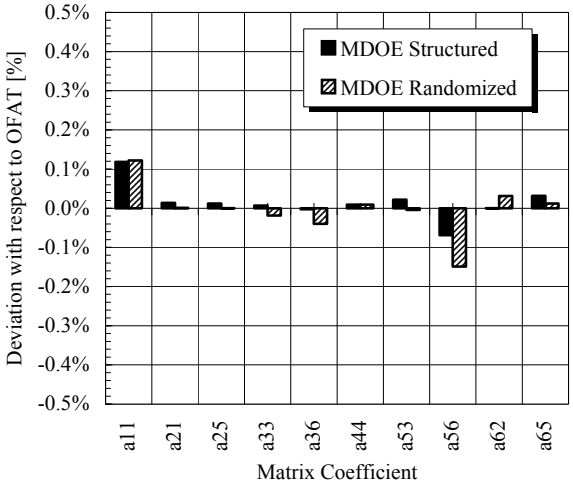

Figure 16. Load table design effect on matrix coef.

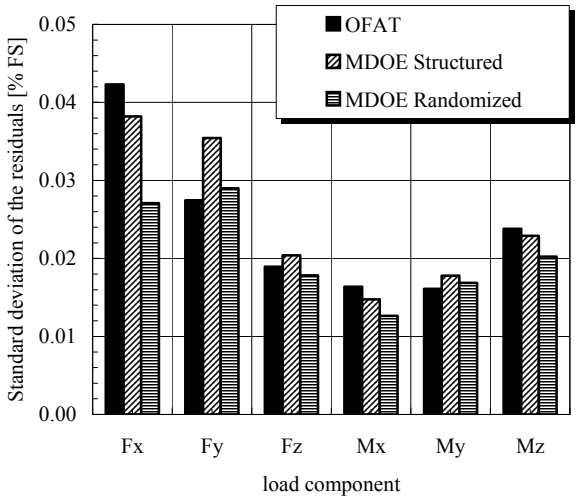

Figure 17. Std. of residuals per calibration

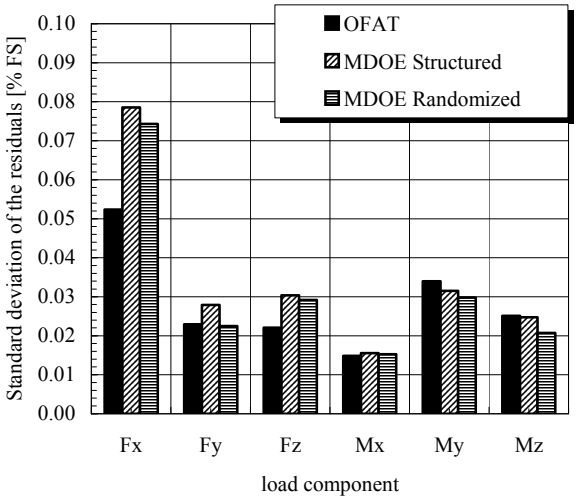

Figure 18. Std. of residuals over the check points

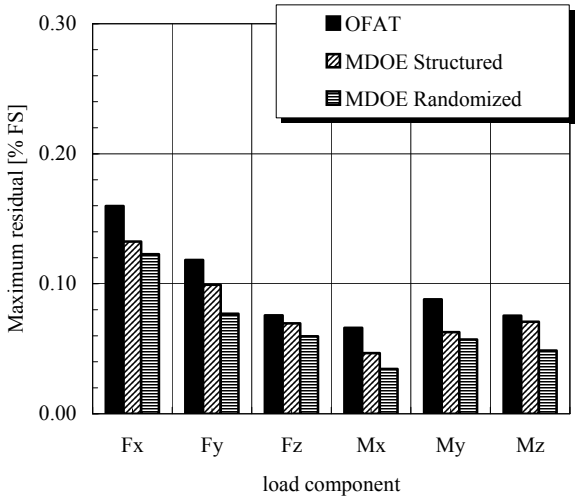

Figure 19. Maximum residual per calibration

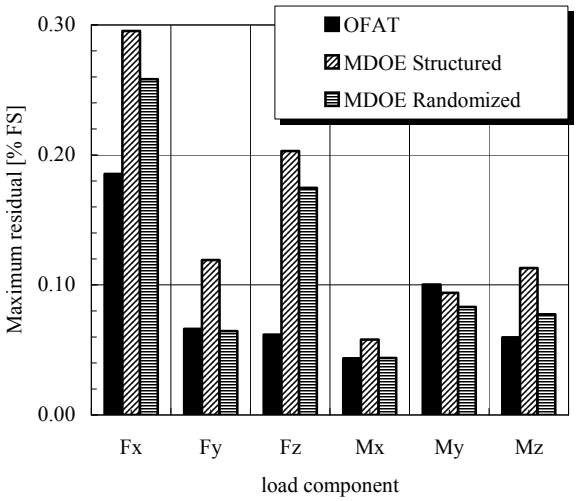

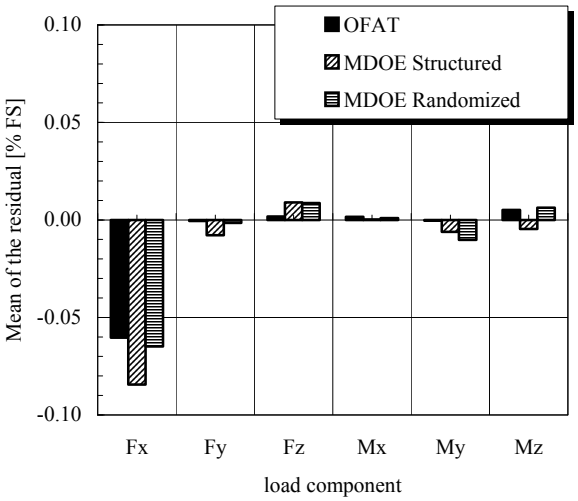

Figure 20. Maximum residual over the check points **Figure 21. Mean of residuals over the check points**

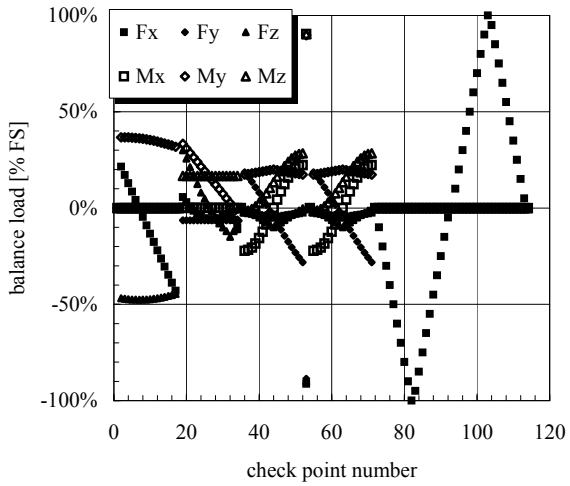

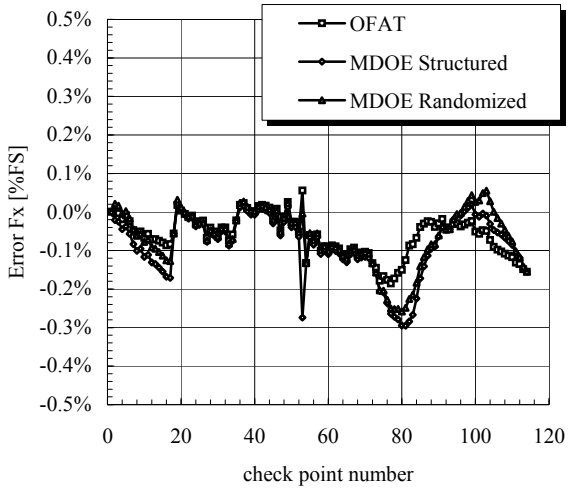

Figure 22. Balance loads for the check load points **Figure 23. Fx residuals for the check load points**

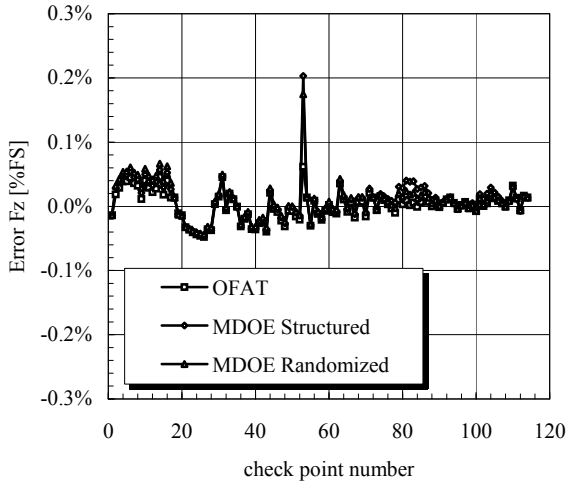

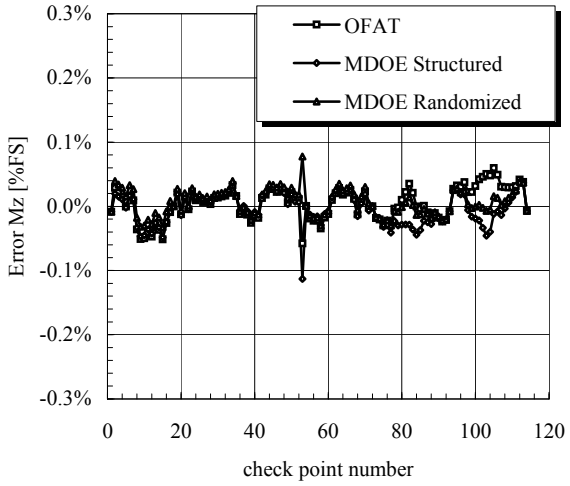

Figure 24. Fz residuals for the check load points **Figure 25. Mz residuals for the check load points**